DEFECTS IN ALUMINUM THIN FILMS DEPOSITED ON PET SUBSTRATE AND THEIR FORMATION MECHANISM

T. Kobayashi[1], I. Yoshifumi[2], Y. Utsumi[3] and H. Kanematsu[4]

[1]Department of Electronics & Control Engineering,
National Institute of Technology, Tsuyama College,
624-1 Numa, Tsuyama, Okayama 708-8509, Japan.

[2]Department of Biochemistry & Applied Chemistry,
National Institute of Technology, Kurume College,
1-1-1 Komorino, Kurume, Fukuoka 830-8555, Japan.

[3]Laboratory of Advanced Science and Technology for Industry,
University of Hyogo, 3-2-1 Kouto, Kamigori-Cho, Ako-Gun,
Hyogo 678-1297, Japan.

[4]Department of Materials Science & Engineering,
National Institute of Technology, Suzuka College,
Shiroko-Cho, Suzuka, Mie 510-0294, Japan.

Corresponding Author's Email: [1]t-koba@tsuyama-ct.ac.jp

Article History: Received 14 December 2018; Revised 25 February 2019;
Accepted 25 April 2019

ABSTRACT: Defects in aluminum films deposited on PET substrate by a vacuum web coater were investigated to clarify their formation mechanisms. The defects detected by optical transmission equipment were taken from a plastic web, and then observed with optical and scanning electron microscopes (SEM). Subsequently, the shapes were classified into four types: teardrop, splashing, scattered dots and round. However, the features of the microstructure were classified as follows: Clear boundary line without films; Unclear boundary line with transparent films; Unclear boundary line with transparent films and residual particles at the center and thermally damaged and penetrated. It has been suggested that the defect formation mechanisms are as follows: (a) splashing of molten aluminum droplets, (b) oxidation of aluminum due to oxygen-containing substances such as water and oil and (c) oxidation of aluminum due to the adhesion of polymer lint.

KEYWORDS: *Aluminum Thin Films; Vacuum Vapor Deposition; Defect; PET Substrate; Splashing*

1.0 INTRODUCTION

Aluminum-coated plastic films (ACPFs) have been widely utilized as packaging materials in the medical, electronics, and foods industries because of their high gas barrier properties [1]. For example, PET films have an oxygen transmission rate (OTR) of around 0.25 [cc/m2/24 h], whereas ACPFs have a much lower OTR of less than 0.005 [cc/m2/24 h] [2]. Furthermore, the water vapor transmission rate (WVTR) of ACPFs is less than one tenth of that of uncoated PET films [3]. Therefore, ACPFs have been used for packaging of potato crisps to prevent them from becoming oxidized, moist, or flavorless, resulting in a long freshness period [4].

ACPFs have been produced by the vacuum deposition of aluminum on a plastic film with a thickness of 12–30 μm using a large-scale vacuum system called a web coater or metallizer [5]. A plastic web having a width of 1–3 m and a rolled length of several thousand meters is used as the substrate and then passed through a cooled drum with a diameter of 0.5–1 m to wind up after vacuum deposition at the cooled drum [5]. The reason for employing a cooled drum is that the plastic film is heated up by heat radiation from the crucible and the latent and sensible heat of the aluminum vapor, resulting in the formation of stripes in the plastic substrate due to permanent thermal deformation or meltdown [6].

There are roughly three types of evaporation source: direct heating, where an aluminum wire is continuously melted in a ceramic composite boat heated with direct electric heating [7]; indirect heating, where an aluminum melted pool is created in a cylindrical or rectangular graphite crucible by heating the crucible with an induction coil [8-10]; and electron beam heating, where aluminum is melted in a water-cooled copper or ceramic crucible by a high-power electron gun [11]. In all types of evaporation, it is widely recognized that so-called “splashing” occurs under inadequate conditions and causes holes in the plastic substrate, resulting in a poor barrier property. Degassing by vacuum melting of evaporation materials and the removal of oxide films on the melting pool are effective in reducing splashing. However, there are few reports or systematic analyses of the defects formed on ACPFs [12].

In the present study, several types of defects formed on aluminum-coated films have been analyzed by optical and electron beam microscopes as reported in a nickel coating [13], and further fundamental verification test has been conducted to clarify the defect formation mechanisms.

2.0 METHODOLOGY

Aluminum coating was performed on a PET substrate with a thickness of 25 μm after surface pretreatment by corona discharge. An air-to-air vacuum deposition system was employed to deposit a 50 nm aluminum film at an evaporation temperature of 1693 K and a web traveling speed of 200 m/min [9]. The defects were detected by optical transmission equipment. As the defects were not always formed, the positions detected were recorded, and then the detected areas of the web were cut off for detailed analysis when the web was used in the subsequent process. The cut substrates were examined by an optical microscope and scanning electron microscopes (SEM; JEOL, JSM-631F), further a part of the defects was analyzed by X-ray photoelectron spectroscopy (XPS; PHI, ESCA 5400 MC).

The samples which deposited aluminum films on PEN substrate were cut then adhered on a sample holder with an electronic conductive tape. Secondary electron images were mainly used for the surface observation. XPS analysis was conducted in a wide scan to investigate the elements on the coating surface with an analyzing diameter of 0.5 mm after ion beam cleaning on the surface.

Fundamental verification experiments were conducted to investigate the causes of the defect formation. Water was added in the deposition room of the web coater by injecting a total amount of 2 cm^3 using a vacuum valve and a medical syringe in an interval of one minute for 3 times, then the affected regions of PET web were sampled after deposition. Machine oil and silicon grease were added by using a small brush at the inlet of the Air-to-Air vacuum pumping system. A piece of plastic sheet having a dimension of 200 mm x 200 mm was kept the deposition plane upside in the operation room where the vacuum web coater has been installed, in order to investigate the effect of dusts, fibers or lint from the environment since the operation room is not a clean room.

3.0 RESULT AND DISCUSSION

3.1 Analysis of the defects obtained

Observation with Optical Microscope

The defects detected by optical transmission while traveling at a speed of 200 m/min exhibited white color recognized as windows. These cut-off defects were observed with the optical microscope and it was clearly confirmed that the optical transmittance was much

higher than that of normal area, though the defects had different shapes. The shapes were classified into four types by the optical microscopy: teardrop, splashing, small dots and string as shown in Figure 1. It was uncertain at this stage whether or not the white windows ha d aluminum films.

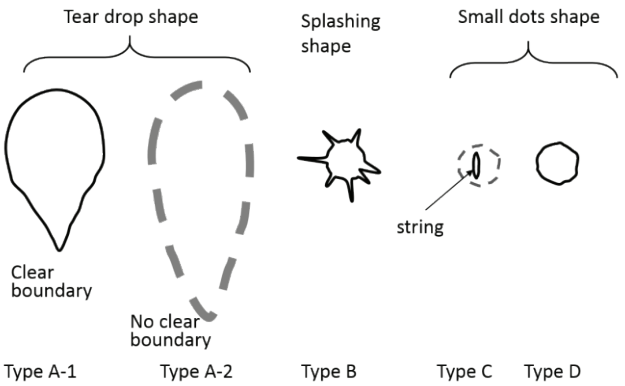

Figure 1: Schematic illustrations of the observed defects by optical microscope

Observations with SEM

Four types of defects were observed by SEM. It was found that the teardrop shape could be divided into two types, one with a clear boundary line and the other with a vague boundary line and cracks in the defect. As shown in Figure 2, regarding the teardrop shape with clear boundary line (Type A-1) having a long axis of 4 mm and a short axis of 2 mm, the aluminum films appeared to become lost or peeled-off in the shape of a teardrop and further peeling was clearly observable at the boundary line. There were no particles or thermal damage on the surface of the substrate. Figure 3 shows the second type of drop shape (Type A-2) with no clear boundary for example, the optical transmittance was gradually increased from the normal area to the defect and neither delamination nor peeling-off was observed by SEM. However, the deposited films were partially cracked and removed at the center of the defect and further concavities, which may have been created by thermal damage were found near the cracks on the substrate. It has not been clarified if the defects were formed by oxidation of the deposited aluminum to aluminum oxide or by decreasing the thickness of the aluminum films.

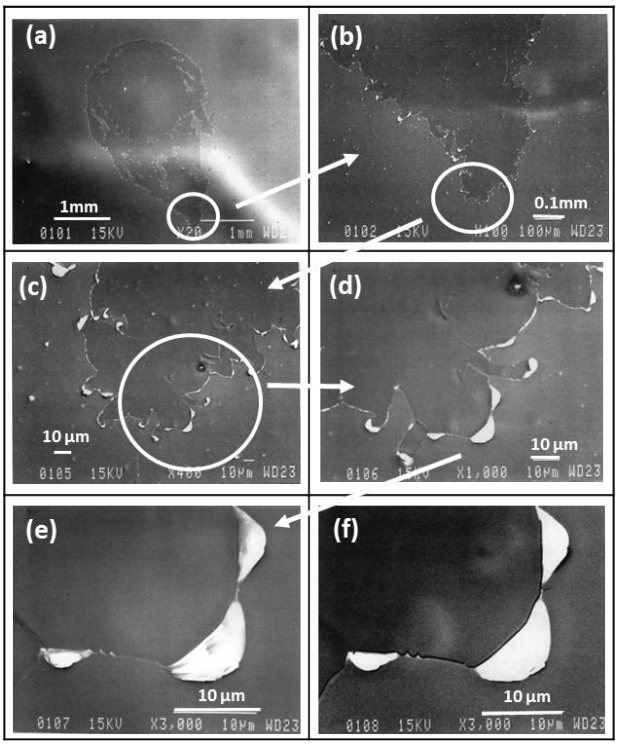

Figure 2: SEM images of a tear drop shape defect (Type A-1): (a)-(e) Defects which observed using secondary electron images and (f) Defects which observed using a reflected electron image

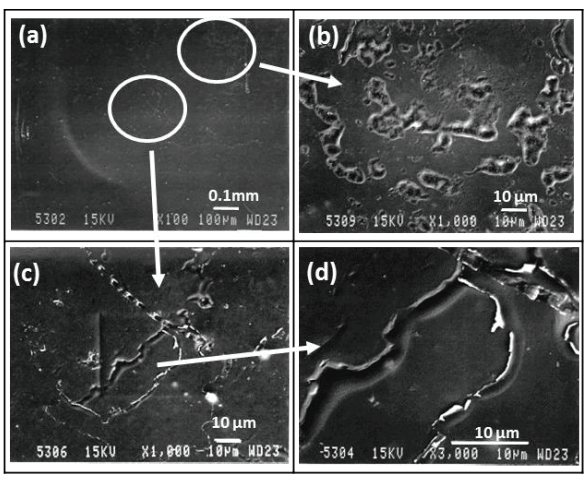

Figure 3: SEM images of a tear drop shape defect (Type A-2): (a)-(d) Defects which observed using secondary electron images

Figure 4 shows an example of splashing shape (Type B). It was suggested that a molten droplet had been hit perpendicularly onto the substrate, and the center area had a round shape and was radially spread outside in many lines. Aluminum was not detected in the defect by XPS as shown in Figure 5 therefore, the aluminum film was either lost or had not formed in the area. Figure 6 shows an example of the small dots shape (Type C). Each dot observed with the optical microscope had a diameter of around 0.5 mm however, it was found that there was a string shape or some other shape possessing length at the center of the dot.

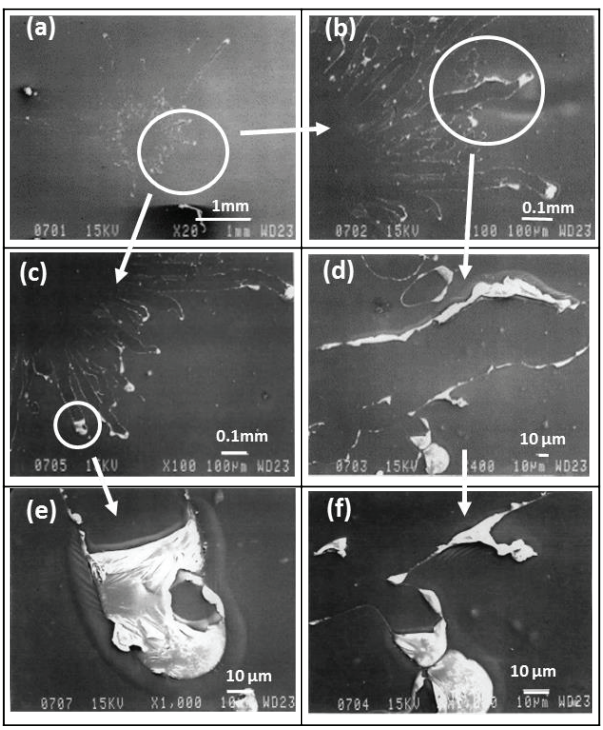

Figure 4: SEM images of a splashing shape defect (Type B): (a)-(f) Defects which observed using secondary electron images

Aluminum was detected by specific X-ray analysis showed that there was no delamination of the deposited aluminum. Some of the defects had particles with diameters of the order of µm at their centers. Figure 7 shows the penetrated shape (Type D). This defect had a hole penetrating the PET substrate or concavities, which could have been formed by heat damage due to colliding particles. The causes for Type A-1 and B, which did not contain aluminum in the defects were supposedly that the aluminum film formation had been prevented, counter-printed, or delaminated because of poor adhesion by the

deposition of water or oil on the substrate or by removal resulting from the occurrence of aluminum droplets. With regard to the Types A-2 and C, which contained aluminum in the defects but exhibited transparency, it has been suggested that the aluminum vapor arriving or aluminum deposited was oxidized to alumina films, thus showing transparency.

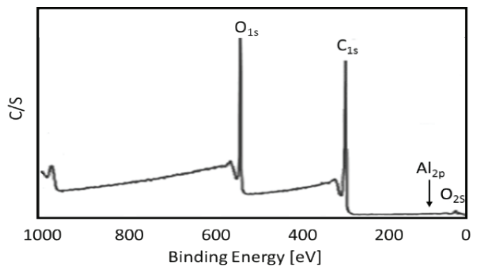

Figure 5: XPS spectrum in wide scan analyzed in the area of a tear drop shape defect (Types A-1 and A-2 in Figure 1)

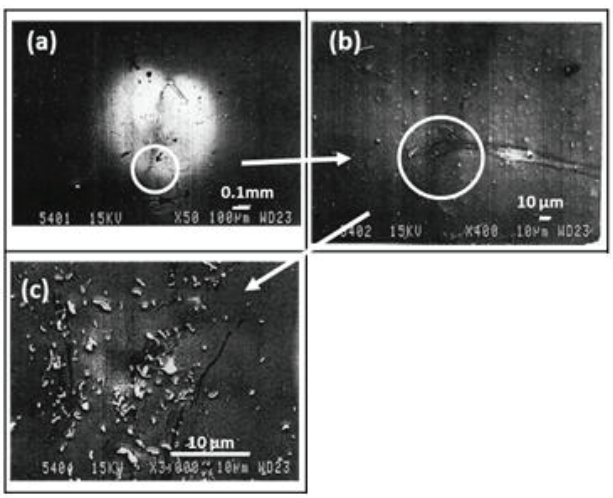

Figure 6: SEM images of a scattered dots shape defect (Type C): (a)-(c) Defects which observed using secondary electron images

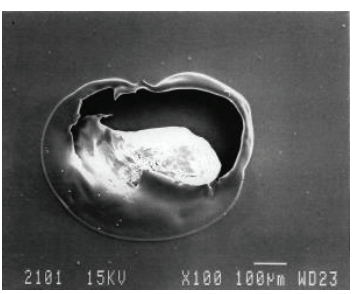

Figure 7: SEM images of a scattered dots shape defect (Type D)

The origin of oxidation was suggested to be the deposition of organic particles or fibers, or the deposition of liquid such as water or oil. The origin of the oxidation of aluminum will be deduced to substances existing in the vacuum coater and substances in taking from environment. Thus water from the leak of cooling water, oils from bearing, organic and inorganic dusts including fibers on plastic substrate are the possible sources for the oxygen. The deductions will be endorsed by a cause investigation experiment in Section 3.2. Furthermore, the thermal damage created by incidental hot materials (shown in Types A-2 and D) and the removal by molten droplets (Types A-1, B, and D) might be caused by splashing from evaporation sources.

3.2 Defects Formation Mechanism

The possible origins are as follows: (1) the deposition of silicon grease used in roll bearings in the vacuum system; (2) the deposition of machine oil used outside the vacuum system; (3) the deposition of water or ice on the cooled drum and (4) the deposition of suspended particles in the room while using or handling the web or on the arrival of molten aluminum droplets from the crucible. In (4), a plastic film placed in the operation room for 24 h was used as the substrate, and aluminum was deposited using bell-jar-type vacuum deposition equipment. Other test specimens were reproduced by the practical metalizer.

The results obtained are shown in Figures 8-12. In Figure 8, the defects that were produced by adding water droplets onto the PET web are shown. Although the shape was neither teardrop nor dot splashing, the defects showed transparency with vague boundaries and cracks. In addition, it was found that the defects contained aluminum by specific X-ray analysis. These features were similar to those of Type A-2 and Type C.

Figures 9 and 10 show the defects created by the addition of mechanical oil and silicon grease. Both showed transparency and finely cracked films, and the shapes were neither teardrops nor dots, but were of relatively large size. The result of the sample kept in the operation room is shown in Figure 11. Large transparent areas were created, the boundaries were not clear, and particles of 1 μm were recognized at the center of the defects. Therefore, it has been suggested that their features were significantly similar to Type C.

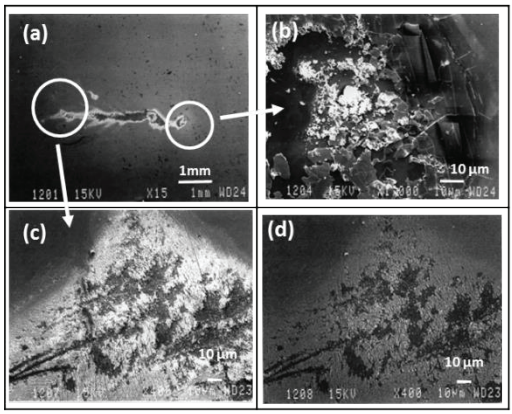

Figure 8: SEM images of a defect produced by adding water droplets onto the PET web: (a)-(c) Defects which observed using secondary electron images and (d) Defects which observed using a reflected electron image

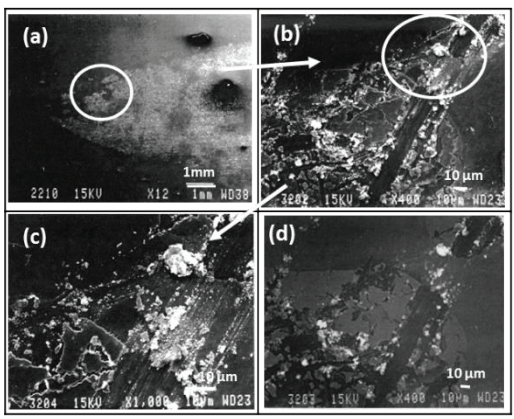

Figure 9: SEM images of a defect created by the addition of mechanical oil onto the PET web: (a)-(c) Defects which observed using secondary electron images and (d) Defects which observed using a reflected electron image

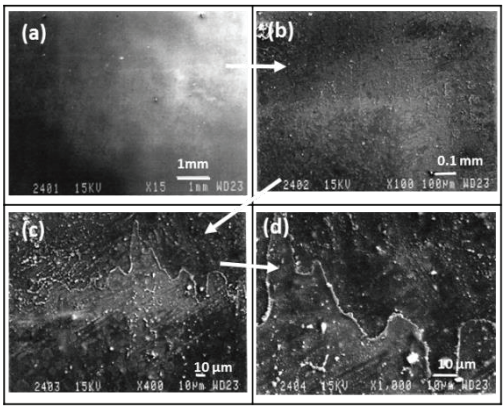

Figure 10: SEM images of a defect created by the addition of silicon grease onto the PET web: (a)-(d) Defects which observed using secondary electrons image

To investigate the effect of splash, molten aluminum droplets or aluminum oxide from the crucible, the relative height of the induction coil to evaporation crucible was varied. It was expected that a higher positioning of the coil would provide a higher temperature at the top of the molten pool than that at the bottom, resulting in a low splashing rate, whereas lower positioning of the coil would result in heavier splashing because of the higher aluminum vapor pressure at the bottom than at the top, resulting in a gaseous phase in the aluminum molten pool. Furthermore, the higher positioning of the coil could cause greater stirring of molten aluminum at the surface area, which could reduce the amount of floating aluminum oxide film, resulting in reduction of splashing.

The defects shown in Figure 12 were obtained with lower positioning, and these results are almost the same as Type A-1. On the other hand, no defects were found with higher coil positioning. These results lead to the following conclusions. Types A-1 and B were created by molten aluminum droplets arriving from the crucible. It has been suggested that the droplets removed the deposited aluminum films or reduced their adhesion to the substrate, resulting in their being transcripted to the backside of the rolled film. Type A-2 was created by the oxidation of aluminum due to the deposition or adhesion of an oxygen-containing substance such as water, silicon grease, mechanical oil, or polymer fiber. Type C was created by the oxidation of aluminum due to the adhesion of polymer fiber. Type D was probably formed by molten aluminum or solid hot particles arriving from the crucible, resulting in thermal damage to the substrate.

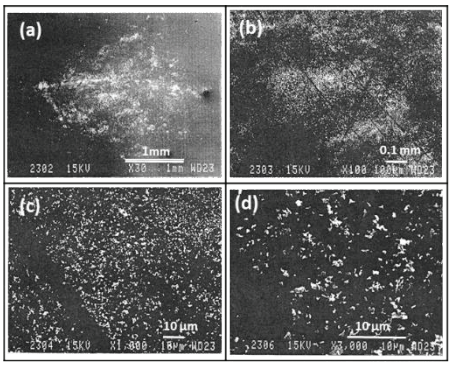

Figure 11: SEM images of a defect formed on the substrate kept in the operation room before deposition: (a)-(d) Defects which observed using secondary electron images

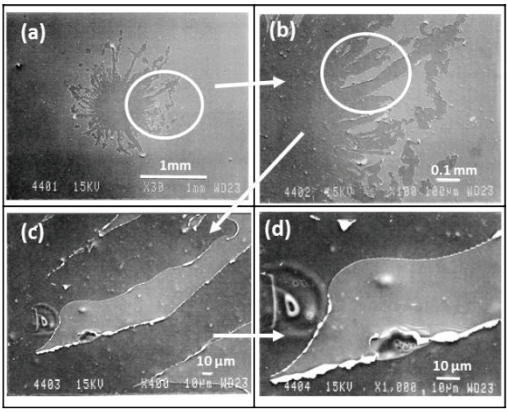

Figure 12: SEM images of a defect obtained with lower positioning of the coil resulting in heavier splashing

4.0 CONCLUSION

The defects formed on aluminum coated polymer web were investigated to clarify the defect formation mechanism, including fundamental verification experiments. It has been concluded that the defects are formed by (a) splashing of molten aluminum droplets, (b) oxidation of aluminum due to the oxygen-containing substances such as water and oil and (c) oxidation of aluminum due to the adhesion of polymer lint.

REFERENCES

[1] R. Mitchell, A. Broomfield, E. Josephson, G. Lobig and P. Raugei, "A Review of Developments in Metallizing Machine Technology", in 41st Annual Technical Conference Proceedings of the Society of Vacuum Coaters, Boston, USA, 1998, pp. 472-476.

[2] J. T. Filts, "Transparent Gas Barrier Technologies", *Journal of Plastic Film and Sheeting*, vol. 9, no. 3, pp. 201-223, 1993.

[3] S. Kanai, N. Yamagishi, C. Ookawara and S. Yoshida, "High Accuracy Measurement of High Moisture Barrier", in 54th Annual Technical Conference Proceedings of the Society of Vacuum Coaters, Chicago, USA, 2011, pp. 641-643.

[4] N. Schiller, S. Straach, M. Fahland and C. Charton, "Barrier Coatings on Plastic Web", in 44th Annual Technical Conference Proceedings of the Society of Vacuum Coaters, Philadelphia, USA, 2001, pp.184-188.

[5] R. Kukla, R. Ludwig and J. Meinel, "Overview on modern vacuum web coating technology", *Surface and Coatings Technology*, vol. 86, pp. 753-761, 1996.

[6] C. A. Bishop and E. M. Mount III, *Metallizing Technical Reference, Fifth Edition*. Fort Mill, SC: The Association of International Metallizers, Coaters and Laminators, 2012

[7] J. Meinel, H. Grimn, W. Schwarz, W. Buschbeck and T. H. Gebele, "Dynamics and Efficiency Aspects in the Evaporator Zone of Vacuum Metallizers", in 36th Annual Technical Conference Proceedings of the Society of Vacuum Coaters, Dallas, USA, 1993, pp.191-196.

[8] Y. Itoh, "High Barrier Film", *Convertech*, vol. 499, no. 10, pp. 109-117, 2014.

[9] T. Taguchi, S. Kamikawa, Y. Itoh, K. Matsuda and M. Mitarai, "Air-To-Air Metallizer: Design and Operational Data", in 35th Annual Technical Conference Proceedings of the Society of Vacuum Coaters, Baltimore, USA, 1992, pp. 135-134.

[10] T. Taguchi, S. Kamikawa, Y. Itoh, K. Matsuda and M. Mitarai, "Air-To-Air Metallizer", in 35th Annual Technical Conference Proceedings of the Society of Vacuum Coaters, Baltimore, USA, 1992, pp. 424-426. 1992.

[11] S. Schiller, U. Heisig and S. Panzer, E*lectron Beam Technology*. New York: John Wiley and Sons, 1982.

[12] C. A. Bishop, *Vacuum Deposition onto Webs, Films and Foils (Second Edition)*. Waltham, USA: Elsevier.

[13] I. S. Othman, M. J. Starink and S. C. Wang, "Impact of Single and Double Zincating Treatment on Adhesion of Electrodeposited Nickel Coating on Aluminum Alloy 7075", *Journal of Advanced Manufacturing Technology*, vol. 12, no. 1(3), pp. 179-192, 2018.